Desalination and Water Treatment
www.deswater.com

doi: 10.5004/dwt.2018.22602

128 (2018) 106–118
October

Polyethersulfone ultrafiltration membranes modified with hybrid Ag/titanate nanotubes: physicochemical characteristics, antimicrobial properties, and fouling resistance

Sylwia Mozia*, Manu Jose, Paulina Sienkiewicz, Kacper Szymański, Dominika Darowna, Michał Zgrzebnicki, Agata Markowska-Szczupak

Faculty of Chemical Technology and Engineering, Institute of Inorganic Chemical Technology and Environment Engineering, West Pomeranian University of Technology, Szczecin, Pułaskiego 10, 70-322 Szczecin, Poland, Tel. +48 91 449 47 30; email: sylwia.mozia@zut.edu.pl (S. Mozia)

Received 15 April 2018; Accepted 30 May 2018

ABSTRACT

The influence of the addition of Ag-modified titanate nanotubes (Ag/TNTs) on transport, antifouling and antibacterial properties of polyethersulfone (PES) ultrafiltration membranes is presented and discussed. The membranes were prepared by the wet phase inversion method using blending of casting dope with Ag/TNTs of various Ag content (2.83 (Ag/TNT_2.5)–23.21 wt% (Ag/TNT_100)). The nanocomposites exhibited good stability in aqueous medium with less than 0.82% of the initial Ag content released during 7 d. The presence of the Ag/TNTs contributed to changes of the surface properties of the membranes evaluated on a basis of zeta potential measurement and atomic force microscopy analysis. Moreover, the modified membranes exhibited higher hydrophilicity than the unmodified (M1) membrane. The addition of Ag/TNTs containing 11.44 or 23.21 wt% Ag contributed to an increase of pure water flux compared with the one measured for M1 membrane, by 15% and 30%, respectively. The applied modification also resulted in an improvement of fouling resistance of the membranes as evaluated on a basis of ultrafiltration of bovine serum albumin solution. Moreover, an improved inhibition of *Escherichia coli* growth with increasing concentration of Ag in Ag/TNTs applied for membrane modification was also observed.

Keywords: Ag; Titanate nanotube; Antibacterial properties; Fouling; Polyethersulfone

1. Introduction

Membrane technology has been identified as an attractive method for water and wastewater treatment [1]. Despite numerous advantages such as high product quality, low energy and space requirements, minimum chemicals usage, continuous automatic operation or easy scaling-up, membrane techniques also exhibit some drawbacks. Amongst them membrane fouling is the primary issue to be addressed adequately, because this undesired phenomenon predominantly reduces the permeability of a membrane and it can lead to its damage. Fouling arises from the interactions of a membrane with organic compounds, colloids, salts, etc., both, on the surface and inside the pores. Furthermore, the accumulation of feed components on the membrane surface creates favorable conditions for a growth of microorganisms resulting in biofilm formation [2–4].

Polyethersulfone (PES) is one of prevalent ultrafiltration (UF) membrane material due to its excellent chemical and thermal stability, mechanical properties, oxidation tolerance, and simple processing [5–7]. However, the low hydrophilicity of PES membranes results in their proneness to fouling and biofouling [5,8]. It is well established that physical and chemical modification of polymeric membranes helps to

* Corresponding author.

Presented at the XII Scientific Conference "Membranes and Membrane Processes in Environmental Protection" – MEMPEP 2018 13–16 June 2018, Zakopane, Poland.

increase their hydrophilicity. Surface modification with polyethylene glycol, polyvinyl alcohol, dendrimers, different block-co-polymers, etc. has been found to limit the attachment of biopolymers and bacterial cells to the membrane [9]. However, these modifications do not remove the formed biofilms, and the membranes suffer from biofouling during the long-term applications. Hence, a development of an antibacterial membrane without altering its initial permeability is of a great importance.

Recently, the blending of various polymers with inorganic nanoparticles (NPs) has emerged as a promising solution to overcome the fouling and biofouling problem [10]. Among the numerous available nanomaterials, silver nanoparticles (Ag-NPs) have gained much interest peculiarly due to their prominent antibacterial properties, less restraint strain formation, and low biotoxicity, and have been found to be very active against a broad spectrum of bacteria [8,11]. Even though the exact mechanism of action of Ag-NPs against bacteria is still under debate, it is widely accepted that the bactericidal activity arises from the release of Ag^+ ions, which next attract to the bacteria surface by electrostatic mechanism and then penetrate through the membrane cell. Inside the cell, Ag^+ ions interact with the thiol groups (S–H) of the bacterial protein resulting in their inactivation [3,12]. Various studies indicate that incorporation of Ag-NPs into the polymer matrix can be effective in reducing the membrane biofouling [13–16]. In situ formation of Ag-NPs on the surface of thin film composite (TFC) reverse osmosis (RO) membrane was used by Ben-Sasson et al. [17]. They reported that the modified membrane exhibited a significant increase of antimicrobial activity compared with the neat one, with only a slight decrease of water permeability. The reduction in the number of living bacteria on the membrane surface evaluated for three model bacteria strains (*Escherichia coli*, *Pseudomonas aeruginosa*, and *Staphylococcus aureus*) exceeded 75%.

Nonetheless, it is also reported that high agglomeration tendency and low stability of the Ag-NPs are the ruling factors, which cause the depletion of antibacterial activity of the composite membranes [3,8]. The surface loading of Ag-NPs onto a suitable substrate, especially on other nanomaterials, has been progressed as an excellent method to enhance its antibacterial performance [18,19]. Nanocomposites of Ag-NPs with multiwalled carbon nanotubes (MWCNTs) [8], silica (SiO_2) [20,21], halloysite nanotubes [10,22], zeolites [23], graphene oxide [24], and sodium zirconium phosphate [13] have been found to show very good antibacterial properties and enhance the biofouling control of the membranes. Ag-NPs can be also incorporated or deposited on titania or titanate nanotubes (TNTs) [25–38].

One-dimensional TNTs have gained much attention due to their unique physicochemical and electronic characteristics, favorable bioactivity, and antifouling properties [25–27]. Their layered structure, high surface-to-volume ratio, oxygen vacancies, and structural defects are advantageous to act against microorganisms [28]. Several studies have explored the significance of Ag/AgO modification of TNTs to improve their antibacterial, antifouling, and photocatalytic performance [20,26,28–31]. There are numerous methods such as photochemical deposition [13,28–31], ion exchange [31], and hydrothermal [32], which have been investigated to modify TNTs with Ag-NPs in order to improve catalytic, antibacterial, and antifouling properties. He et al. [39] applied the surface coating of TNTs with Ag-NPs based on the traditional silver mirror reaction for preparation of anode material for lithium–ion battery. Wei et al. [12] pointed out that TNTs act as a nanocontainer for the storage and allow for the controlled release of Ag through diffusion and osmosis effect.

Recently, modification of polymer membranes with TNTs has been found to be effective in enhancing permeability, hydrophilicity, and antifouling properties [33–37]. Padaki et al. [35] attributed this enhancement to the large number of hydroxyl groups present on the surface of the TNTs, which helped to enrich hydrophilicity of the modified membrane. Modified TNTs may also be incorporated into the polymer membranes. Azelee et al. [38] prepared TFC-RO membrane with MWCNT-TNT nanocomposite, and the modified membrane was found to exhibit improved both, flux and salt rejection. Alsohaimi et al. [36] studied the effect of sulfonic acid functionalized TNTs on polysulfone (PSU) UF membrane properties and revealed that the modified membrane showed good antifouling and separation properties.

To the best of our knowledge, there is lack of information on the possibilities of application of Ag/TNTs to improve permeability and biofouling resistance of PES UF membranes. Hence, we have proposed fabrication of novel mixed matrix membranes by blending PES with various Ag/TNTs synthesized via photodeposition approach. The morphology, structure, and stability of the nanomodifiers and membranes are discussed in detail. Moreover, the transport characteristics of the membranes, evaluated on the basis of the pure water flux (PWF), are presented. Furthermore, the antifouling performance with reference to bovine serum albumin (BSA) UF is described. Finally, the antibacterial properties of the Ag/TNTs and the modified membranes against *E. coli* bacteria are demonstrated.

2. Experimental

2.1. Materials

PES was provided by BASF, Germany. Anatase TiO_2 powder was purchased from Sigma-Aldrich Chemicals, USA. *N,N*-dimethylformamide (DMF), ammonium sulfate, hydrochloric acid (35–38 wt%), silver nitrate, sodium hydroxide, and sulfuric acid (96 wt%) were purchased from Avantor Performance Materials, Poland S.A. BSA (Probumin) was purchased from Merck, Germany.

Microbiological tests were carried out using Plate Count Agar (PCA; BIOCORP, Poland). NaCl was provided by Chempur (Poland). Gram negative *E. coli* (strain K12, ATCC 29425, USA) bacteria were used as model microorganisms. The initial concentration of bacteria suspension was set at 0.5 using McFarland scale (McFarland standards, bioMérieux, France). Whatman™ qualitative filter papers (GE Healthcare UK Limited, UK), grade 1, were used in the diffusion inhibition zone tests.

In all experiments pure (deionized) water (type 2, 0.066 μS/cm) from Elix 3 (Millipore) was used, unless otherwise stated.

2.2. Preparation of TNTs

TNTs were prepared by employing hydrothermal treatment of anatase TiO_2 powder. Initially, TiO_2 (2 g) was ultrasonicated with 60 cm^3 of 10 M NaOH solution for 1 h at room temperature to obtain a homogeneous dispersion. The dispersion was then transferred to a Teflon-lined stainless steel autoclave and then heated at 140°C for 24 h. After being cooled down to room temperature, the mixture was first washed with 2 dm^3 of 0.1 M HCl and then with deionized water until the conductivity of the filtrate became ~1 μS/cm. Finally, the white product was dried at 80°C in an oven for 12 h and stored.

2.3. Preparation of hybrid Ag/TNTs

The Ag-NPs were deposited onto TNTs through photoreduction approach [19]. In a typical reaction, 1 g of TNTs was dispersed into 100 cm^3 of $AgNO_3$ solution (2.5, 10, 50, and 100 mM) with magnetic stirring (250 rpm) for 2 h at ambient temperature and pressure in a glass reactor. Afterwards, the slurry was irradiated with a low pressure mercury vapor lamp (TNN 15/32, Heraeus Noblelight GmbH, 15 W, λ_{max} = 254 nm) for 2 h with continuous stirring. The suspension was then collected by centrifugation and subsequently washed several times with deionized water for the complete removal of excess of Ag^+ ions. Finally, the products were dried at 80°C in an oven for 12 h and stored. The samples were denoted later as Ag/TNT_2.5, Ag/TNT_10, Ag/TNT_50 and Ag/TNT_100, where the numbers represent the concentration of $AgNO_3$ solution.

2.4. Preparation of casting solutions and membranes

The membranes were fabricated using wet phase inversion method under relative air humidity of 20% ± 3%. For the preparation of the casting solutions, PES as a polymer, DMF as a solvent, and water as a nonsolvent were used. The casting dope compositions are presented in Table 1.

The unmodified membrane (M1) was obtained by dissolution of the polymer (8.38 g) in a solvent (50 cm^3), degassing of the solution, and casting of a thin film on a glass plate using the applicator (Elcometer 4340, Elcometer Ltd., UK) equipped with the casting knife (gap set at 0.1 mm). Finally, the casted membrane was immersed in the nonsolvent at the temperature of 20°C for 24 h.

The membranes modified with Ag/TNTs (1 wt% in relation to PES) were prepared as follows. At first, a suspension of NPs in solvent (10 cm^3) was sonicated for 30 min using ultrasonic liquid processor (Vibra-cell VCX-130, Sonics, USA; output power 130 W, frequency 20 kHz, amplitude 80%) equipped with a 6 mm ultrasonic probe. Next, the obtained suspension was added into the PES/DMF (8.38 g/40 cm^3) solution and sonicated in ultrasonic bath (Sonic-6D, Polsonic, Poland; output power 320 W, frequency 40 kHz) at temperature of 20°C–25°C for 15 min and subsequently stirred (200 rpm) at temperature of 55°C–60°C for 15 min. Both steps, that is, sonication and mixing were carried out by turns for 2 h.

Table 1
Composition of casting solutions

Membrane code	Type of NPs	PES:DMF	NPs (wt% in relation to PES)
M1	–	15:85	–
M2	Ag/TNT_2.5	15:85	1
M3	Ag/TNT_10	15:85	1
M4	Ag/TNT_50	15:85	1
M5	Ag/TNT_100	15:85	1

2.5. Characterization of TNTs and Ag/TNTs

The morphology of TNTs and Ag-modified TNTs was investigated using transmission electron microscope (TEM) FEI Tecnai F20. The samples were prepared by sonication in ethanol, after which a drop of the suspension was deposited on a carbon-coated copper grid (300 mesh).

The phase composition of the pure TNTs and hybrid TNTs was examined basing on X-ray diffraction (XRD) method (PANalytical Empyrean X-ray diffractometer) using CuKα radiation (λ = 1.54056 Å).

The concentration of Ag in the hybrid NPs was evaluated by inductively coupled plasma optical emission spectrometry (ICP-OES) method using Optima 5300DV spectrometer (Perkin Elmer, USA). Before analysis, the Ag/TNTs samples were dissolved in a hot solution of $(NH_4)_2SO_4$ in a concentrated H_2SO_4. Then the solution was cooled down and diluted with water.

The Ag release profiles from Ag/TNTs nanocomposites with the lowest (Ag/TNT_2.5) and the highest (Ag/TNT_100) concentration of Ag were measured during 7 d period. For this experiment, 200 mg of Ag/TNT_2.5 and Ag/TNT_100 nanocomposites were dispersed into 200 cm^3 of deionized water and placed in a digital shaking water bath operated at 30°C. A defined amount of samples was withdrawn at a predetermined time interval and separated through a 0.45 μm filter. The concentration of Ag in the filtrate was analyzed using ICP-OES spectrometer.

The isoelectric point pH(*I*) of the Ag/TNTs nanocomposites was assessed using Zetasizer Nano-ZS (Malvern Instruments Ltd., UK) equipped with Multi Purpose Titrator MPT-2 and a degasser. The samples were dispersed in ultrapure water and the pH was adjusted using HCl and NaOH solutions.

2.6. Characterization of membranes

The isoelectric point of the membranes was evaluated using SurPASS 3 analyzer (AntonPaar, Austria). The solution of 0.001 M KCl in ultrapure water (Simplicity, Millipore) was applied as an electrolyte. The pH was adjusted using HCl and KOH solutions. The pH(*I*) was calculated as a mean from at least two repeated measurements.

The porosity was determined using gravimetric analysis and calculated on a basis of the Eq. (1) as follows:

$$P = \frac{\left(m_{\text{wet}} - m_{\text{dry}}\right)/\rho_w}{\left(m_{\text{wet}} - m_{\text{dry}}\right)/\rho_w + m_{\text{dry}}/\rho_p} \times 100\% \quad (1)$$

where m_{wet} and m_{dry} are the weight (g) of membrane samples in the wet and dry state, respectively; ρ_w is water density at

20°C (ρ_w = 0.9982 g/cm^3); and ρ_p is the PES density (1.37 g/cm^3). The given values were obtained from three independent measurements.

The water contact angle of the membranes was measured by putting a sessile water drop (10 μL) on the membrane surface and collection of the results using the goniometer model 260 (ramé-hart instruments co., USA). The contact angle values were calculated as an average of at least 10 measurements from 3 different membrane pieces.

The topography of the membranes surface was examined using atomic force microscopy (AFM). NanoScope V Multimode 8 scanning probe microscope (Bruker Corp., USA) was applied. The measurements were carried out with the silicon nitride ScanAsyst – Air probe in the ScanAsyst mode, which used the so-called Peak Force Tapping Mechanism. The scanned surface was 10 μm × 10 μm.

The surface and the cross-section of the membranes were investigated using Hitachi SU8020 Ultra-High Resolution Field Emission Scanning Electron Microscope (SEM). Before analysis, the membranes were dried in a series of soaking solutions consisting of water and ethanol in concentrations of 0, 20, 40, 60, 80, and 96 vol.% of ethanol. For the cross-sections measurements, the membranes were immersed and crushed in liquid nitrogen. Before analysis, the membrane samples were mounted on a table using carbon tape and coated with a 5 nm thick chromium layer (Q150T ES coater, Quorum Technologies Ltd., UK). Two types of measurement techniques were used, that is, analysis using secondary (SE) and back scattered electrons (BSE). The accelerating voltage was 5 and 15 kV for SE and BSE, respectively.

Ag^+ release from membranes was examined on the basis of leaching tests of the procedure as follows. Membrane samples (total area of 56.25 cm^2), previously dehydrated in the ethanol soaking solutions and dried in the air were inserted into the Duran glass bottles containing 100 cm^3 of NaCl saline solution (8.5 g NaCl/dm^3) and a stirrer bar. Subsequently, the bottles were put into incubator and stirred at 250 rpm for 7 d. Ag content in the solutions was evaluated basing on ICP-OES measurement using Optima 5300DV spectrometer (Perkin Elmer, USA).

The laboratory scale membrane installation was applied during UF experiments. The installation consisted of a suction pump with a pressure dampener, a stainless steel membrane module (with a 1.194 mm feed spacer), a manometer, and a needle valve. The membrane working area was 0.0025 m^2. The transmembrane pressure (TMP) of 1, 2, or 3 bar was used for determination of the PWF. The temperature was set at 20°C ± 1°C. Each experiment was carried out at least four times.

The influence of Ag/TNTs on membrane fouling was evaluated based on UF of BSA solution (1 g/dm^3) at TMP = 2 bar and feed cross flow velocity of 1 m/s. The concentration of BSA in feed (C_f) and permeate (C_p) was determined using the total organic carbon analyzer (multi N/C 3100, Analytik Jena, Germany). The rejection coefficient (R) was calculated on the basis of Eq. (2) as follows:

$$R = \frac{C_f - C_p}{C_f} \times 100\% \quad (2)$$

2.7. Microbiological study

2.7.1. Preparation of culture media

First, PCA solution was prepared according to the instructions given by the manufacturer. Next, the Petri dishes were filled with PCA solution and left for solidification. Finally, the prepared agar plates were sterilized under UVC light for 20 min and then dried in an incubator for 3 d.

NaCl saline solution was prepared by dissolving 8.5 g NaCl in 1 dm^3 of the deionized water and then sterilizing in an autoclave.

2.7.2. Bacteria counting

The *E. coli* bacteria were counted using the serial decimal dilutions in NaCl solution. 0.3 cm^3 of a suitable diluted solution was put in the middle of a plate containing PCA and spread using a spreader. Three repetitions for each dilution were prepared. The plates with bacteria were incubated at 37°C for 24 h. After that, the visible colonies of bacteria on agar plates were calculated using the counter (LKB 2002, POL-EKO, Poland). The average Colony Forming Unit (CFU) per cm^3 values were evaluated according to Eq. (3) as follows:

$$\mathrm{CFU/cm^3} = \frac{N \times Y}{Z} \quad (3)$$

where N – number of bacteria colonies visible on Petri dish, Y – total dilution factor, Z – volume of bacteria suspension put on the agar plate (0.3 cm^3).

2.7.3. Antimicrobial activity of Ag/TNTs

Antimicrobial activity of Ag/TNTs was measured using the disk diffusion method. First, the *E. coli* bacteria were spread on the Petri dishes containing PCA culture medium. Then, sterile paper disks (22 mm diameter), previously sonicated for 10 min in a 1 g/dm^3 suspension of defined NPs in saline solution, were placed on the dishes. Before usage, the suspension was sonicated for 30 min using ultrasonic bath. The Petri dishes were incubated at 37°C for 24 h. After that time the inhibition zones were measured.

2.7.4. Study of antimicrobial activity of the membranes

At first, a piece of a membrane (12.5 cm × 4.5 cm) was cut and dehydrated in a series of ethanol soaking solutions and dried in the air as described previously. Subsequently, the membrane sample was put into a Duran glass bottle containing 100 cm^3 of bacteria suspension in NaCl saline solution (turbidity of 0.5 according to McFarland scale). Then, an ellipsoidal stirrer (diameter 12 mm, length 25 mm) was put inside the bottle. The bottle was closed and put on a magnetic stirrer (250 rpm) at 37°C for 40 h. After the incubation, three samples were taken from each bottle and the antimicrobial activity of the membranes was calculated using the dilution method described earlier. The control (blank) test was prepared under the same conditions, but without addition of a membrane inside the bottle. The percentage of the

inhibition of bacterial growth was calculated with reference to the control (blank) sample according to Eq. (4) as follows:

$$I\% = \left(\frac{(B - C)}{B} \right) \times 100\% \quad (4)$$

where: B – amount of bacteria determined in the control sample (CFU/cm^3), C – amount of bacteria determined in the presence of a membrane [CFU/cm^3].

3. Results and discussion

3.1. Characterization of TNTs and Ag/TNTs nanocomposites

The microstructure of the unmodified and Ag-deposited TNTs was determined by TEM and the corresponding images are presented in Fig. 1. Fig. 1(a) shows that unmodified TNTs exhibited well dispersed, multi-walled and open-ended nanotubular morphology with length of approximately 50–200 nm and the inner diameter of 6–8 nm. TEM image of Ag/TNT_100 is presented in Fig. 1(b). The Ag-NPs were found to be uniformly distributed on TNTs and the corresponding energy-dispersive X-ray (EDX) spectrum shown in the inset of Fig. 1(b) confirmed the presence of Ag-NPs. A majority of Ag-NPs exhibited the size of 2–5 nm, however, some single NPs with diameters as large as 12–15 nm were also observed.

Based on the XRD patterns of TNTs and Ag/TNTs (data not shown), hydrogen titanate ($H_2Ti_3O_7$) with a small fraction of anatase phase was identified in the samples. Nonetheless, regardless of $AgNO_3$ concentration used for sample modification, the presence of metallic Ag or silver oxides (Ag_2O or AgO) was unable to be identified from XRD patterns, which was probably due to too low content of these species. The amount of Ag in the different nanocomposites measured by ICP-OES analysis is presented in Table 2. The weight fraction of Ag in the nanocomposites was found to increase with the increase in the initial concentration of $AgNO_3$.

Table 2
The amount of Ag in different Ag/TNTs nanocomposites measured by ICP-OES

Sample name	Ag (wt%)
Ag/TNT_2.5	2.83
Ag/TNT_10	7.26
Ag/TNT_50	11.44
Ag/TNT_100	23.21

3.2. Ag^+ release study from Ag/TNTs nanocomposites

In order to evaluate the stability of Ag/TNTs nanocomposites, the leaching tests were realized using the samples containing the lowest and the highest Ag amount. The quantity of Ag^+ ions released from Ag/TNT_2.5 and Ag/TNT_100 nanocomposites into the water during 7 d period is illustrated in Fig. 2.

The Ag/TNT_100 showed comparatively higher Ag^+ ion release than Ag/TNT_2.5 which was directly related to the amount of Ag present initially in the nanocomposites. Moreover, a steady increase in the release of Ag^+ ions was observed for Ag/TNT_100 reaching 0.82% of the initial Ag content in the nanocomposite (Table 2) after 7 d. The release of Ag^+ from the Ag/TNT_2.5 nanocomposite was initially below the detection limit of the method (0.01 mg/dm^3 for Ag) and in the last 2 d of the experiment the concentration of silver in water reached 0.04% of the initial content in the nanocomposite (Table 2). The obtained results suggest significantly lower leaching of Ag^+ from Ag/TNT_2.5 than from Ag/TNT_100. As observed in Fig. 1, the surface of the titanate

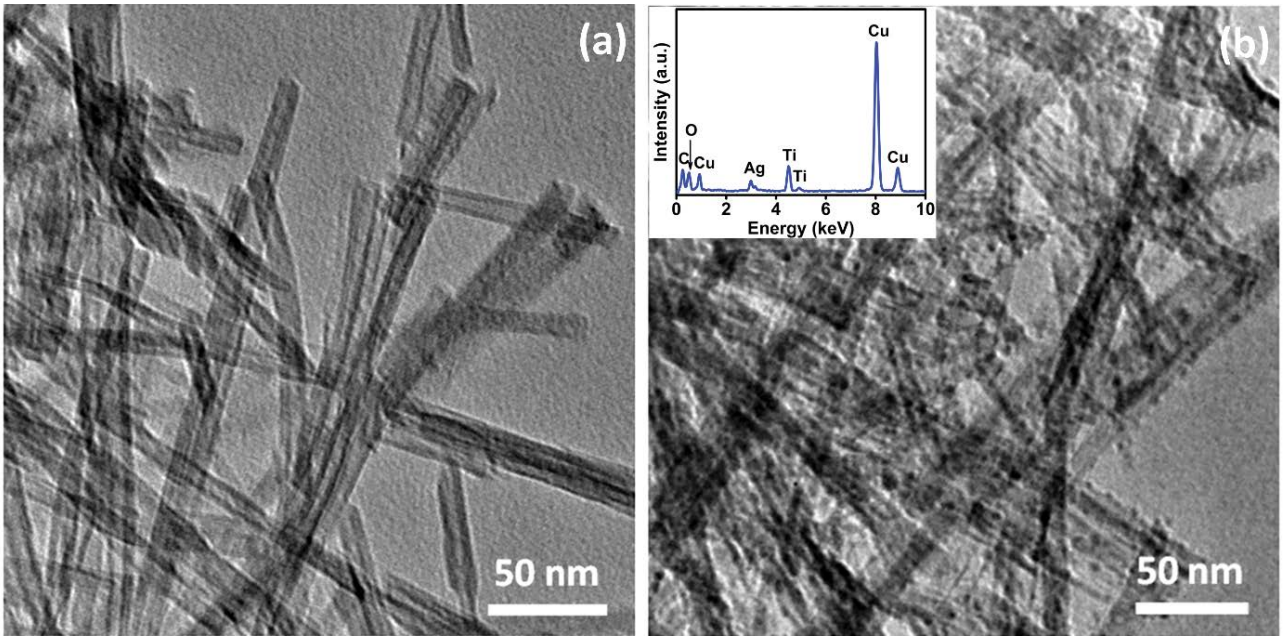

Fig. 1. TEM images of (a) pure TNTs and (b) Ag/TNT_100; the inset shows EDX pattern of Ag/TNT_100.

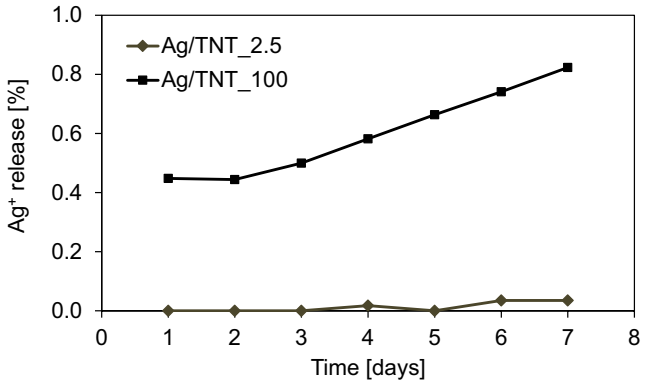

Fig. 2. The silver release profile of Ag/TNT_2.5 and Ag/TNT_100 in water during 7 d of leaching test. Values calculated with reference to the initial Ag content in the nanocomposites.

nanotube was thoroughly covered with Ag-NPs and this oversaturation resulted in the elevated leaching of Ag^+ ions from Ag/TNT_100.

3.3. Antibacterial assay of Ag/TNTs nanocomposites by disk diffusion method

The main focus of this study was to develop an UF membrane with improved antibiofouling properties by incorporation of Ag/TNTs as an antibacterial agent. Keeping this in mind, the antibacterial properties of the nanofillers were qualitatively assessed using disk diffusion method in the dark against Gram-negative (*E. coli*) bacteria. Fig. 3 shows the results obtained after 24 h of incubation.

In case of all samples, the well-defined inhibition zones were observed. The diameter of zones was ca. 27 mm, regardless of Ag content in the nanomaterial, showing that even at the lowest amount of silver deposited on TNTs, the hybrid NPs revealed antibacterial activity. The positive influence of the presence of Ag photodeposited on TNTs on the antibacterial properties of the hybrid nanomaterial was also reported by Viet et al. [19] in the experiments with *S. aureus*. The observed in Fig. 3 action of the Ag/TNTs can be attributed to the release of Ag^+ ions, being antibacterial agents, from the nanocomposites [40]. Although the mechanism of antimicrobial effects of silver is still not fully understood [40], it is commonly accepted that the interaction of Ag^+ with thiol groups plays the essential role in bacterial inactivation. It was also postulated that silver can penetrate bacterial cells and cause damage by interacting with DNA, molecules of which become more condensed and lose their replication abilities [40,41]. Moreover, it was proposed that after penetration Ag can inactivate the bacterial enzymes, thus increasing the production of hydrogen peroxide and leading to cell death [41]. Furthermore, Ag-NPs are believed to attach to the surface of the cell membrane and disturb its permeability and respiration [41]. In such a case smaller particles with a larger surface area may have stronger antibacterial potential than greater ones [41].

3.4. Characterization of Ag/TNTs nanocomposite membranes

Table 3 presents selected physicochemical properties of the fabricated membranes. For all the prepared membranes the calculated value of porosity was 70%–72%. Although NPs are considered as pore-forming agents, the low concentration of Ag/TNTs applied in the discussed experiments (1 wt% with reference to PES) did not contribute to any significant changes of the discussed parameter.

The incorporation of Ag/TNTs in the membranes structure resulted, however, in an increase of their hydrophilicity (Table 3). The unmodified M1 membrane exhibited higher values of contact angle (54°) than the membranes modified with Ag/TNTs (47°–48°). Nonetheless, the differences between M2 and M5 membranes were not significant, which may have been due to the same amount of nanomaterials used for membranes modification (1 wt% in relation to PES).

Fig. 4 presents stabilized PWFs measured for various membranes at TMP = 1, 2, and 3 bar. The analysis of permeability revealed that the addition of Ag/TNTs into the casting solution had significant influence on water transport properties of the prepared membranes. In case of the membranes with low concentration of Ag (M2 and M3), the addition of the nanomodifiers resulted in a slight (ca. 10%) decrease of PWF in comparison with the unmodified membrane (M1). However, when the silver content was higher (M4 and M5), an improvement of PWF compared with the neat (M1) membrane was observed. The permeability of the M4 membrane was higher by ca. 15% than one observed for M1, and in case of M5 membrane ca. 30% improvement was noted.

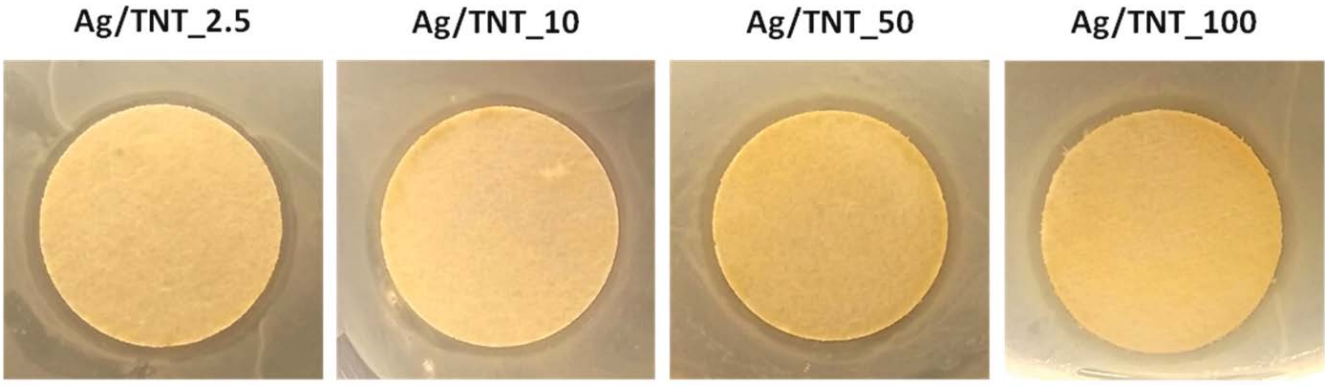

Fig. 3. Photographs of the zone of inhibition observed for various Ag/TNTs against *E. coli*.

Table 3
Physicochemical properties of membranes

Membrane	M1	M2	M3	M4	M5
Contact angle (°)	54	47	47	48	48
Isoelectric point (–)	3.6	3.5	3.4	3.1	3.4
Porosity (%)	70	71	71	71	72

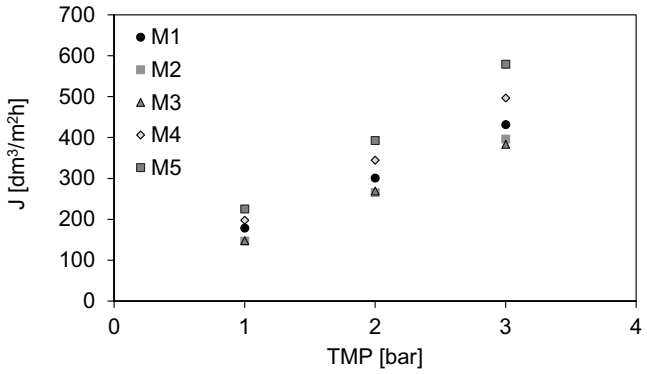

Fig. 4. The influence of the type of Ag/TNTs on pure water flux of PES membranes.

It is reported in the literature that the incorporation of Ag-NPs into membrane matrix can change structure and physicochemical properties such as hydrophilicity, porosity, and surface charge of the membranes [42]. However, the reports on the positive and negative aspects of the modification are inconsistent. There are some papers describing a decreased water permeability with increase of Ag concentration in a membrane matrix [14,43]. The authors explained this phenomenon by blockage of membrane pores by Ag-NPs leading to a decrease of water permeation through membrane. Nonetheless, in most of the reports it is claimed that Ag addition can enhance the transport properties of the modified membranes due to the increase of their hydrophilicity. Such a phenomenon has been observed for polyvinylidene fluoride UF membranes modified with Ag-NPs [44] or Ag-TiO_2 NPs [45] as well as in case of PSU membranes modified with pure Ag-NPs [46] or nanocomposite Ag-NPs/polydopamine nanomaterial [47]. The literature data refer also to fabrication of PES membranes via blending and phase inversion method using different nanocomposite fillers containing silver: halloysite nanotubes – chitosan – Ag [22], halloysite nanotubes – Ag [10] and Ag loaded-sodium zirconium phosphate [25]. In all cases, an increase of PWF has been observed, although the magnitude of improvement depended on the nanomaterial used. Furthermore, all researchers associated their results with the increased hydrophilicity of the modified membranes. Moreover, usually an increase of PWF with increasing content of a hybrid Ag-modified nanomaterial (in a certain range, usually up to 3 wt%) has been observed [10,22,25,46].

In case of the membranes presented in this work, the content of Ag/TNTs was kept constant (1 wt% in relation to PES), however, the NPs differed in Ag loading. Thus, the increase of the permeate flux observed in case of M4 and M5 membranes (Fig. 4) could be attributed to the concentration of Ag in the nanomaterial (Table 2). Such conclusion can be supported by the literature data reporting a positive influence of increasing Ag-NPs content on a membranes permeability [46,48].

Fig. 5 presents the SEM microphotographs of the membranes cross-sections. All the membranes exhibited asymmetric structure with a thin skin layer. The finger-like, oblong pores visible in the entire cross-section of the prepared membranes narrowed toward the upper membrane surface. In the bottom part of the cross-section, some pores resembling bubbles could be also observed. The large pores were accompanied by a sponge-like structure, visible especially in the bottom part of the membrane cross-section.

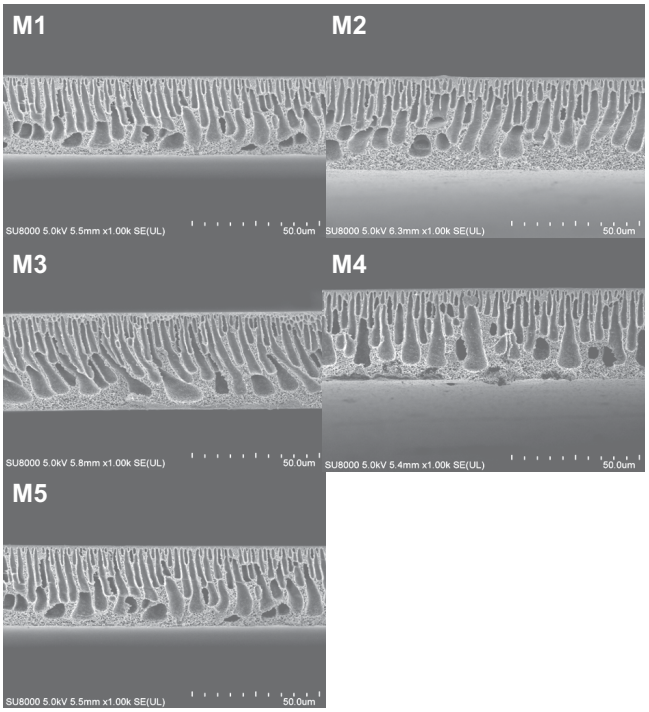

Fig. 5. SEM cross-section images of the fabricated membranes.

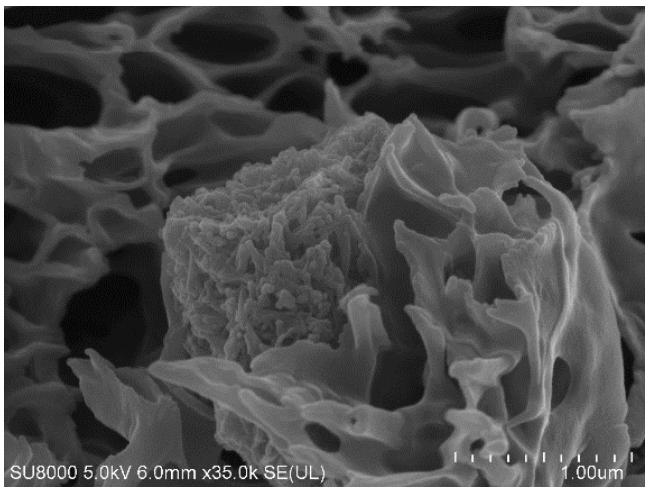

Fig. 6. SEM image of Ag/TNT_2.5 agglomerate in the M2 membrane.

A more detailed SEM analysis revealed the occurrence of Ag/TNTs agglomerates localized at a various depth of the mixed-matrix membranes cross-sections (Fig. 6).

The size of the agglomerates could be possibly reduced by the application of lower concentrations of the nanomaterial, as was proposed by Sotto et al. [49]. The authors reported a noticeable shift of TiO_2 particle size distribution in a solution of PES in *N*-methyl-2-pyrrolidone to a larger mean diameters as the nanomaterial content increased from 0.035 to 0.125 wt%. Furthermore, they concluded that the presence and the size of NPs aggregates had an influence on their dispersion rate in the membrane matrix and on the surface, as well as on the pore size distribution of the formed membranes. They also observed that the TiO_2 content affected the permeability of the prepared nanofiltration membranes, which was the highest at 0.085 wt% of nanomaterial. At higher concentrations, a slight decrease in permeability was found and it was attributed to pore blockage and a decrease in the average pore size [49]. The membranes presented in this work contained a constant loading of Ag/TNTs equal to 1 wt% in relation to PES, which was significantly higher than that described by Sotto et al. [49]. That can explain the occurrence of the large agglomerates in the membrane matrix, as presented in Fig. 6. Furthermore, it cannot be excluded that lowering the Ag/TNTs content to similar ultralow values as reported in Ref. [49] could further improve the modified membranes performance.

The presence of Ag/TNTs on the membranes surface was also verified basing on AFM analysis. Fig. 7 shows the topography of the unmodified membrane and the

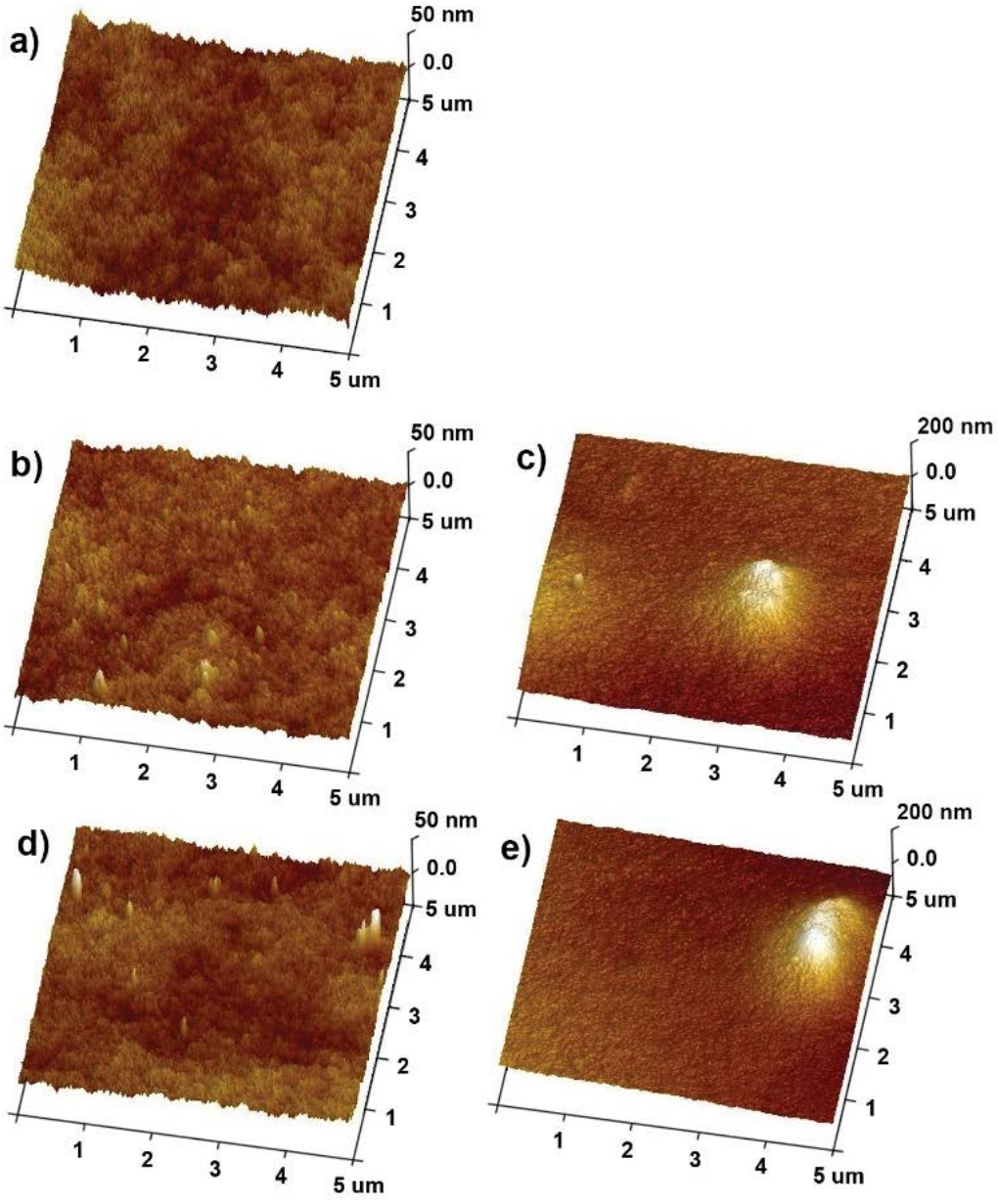

Fig. 7. AFM images of (a) M1 membrane, (b) and (c) M4 membrane, and (d) and (e) M5 membrane.

membranes containing Ag/TNT_50 (M4) and Ag/TNT_100 (M5) nanocomposites. The unmodified membrane had a smooth surface, whereas the membranes modified with NPs exhibited the presence of the smaller (≤0.2 μm) as well as larger (>3 μm) mountain-like irregularities. These various forms present on the surface of the modified membranes could explain the changes in hydrophilicity discussed earlier (Table 3).

One of the factors influencing the performance of membranes in terms of fouling and biofouling is their surface charge. Fig. 8 shows the influence of pH on the zeta potential of the prepared membranes.

The isoelectric point of the unmodified membrane (M1) was little higher than that of the mixed matrix membranes and amounted to pH(*I*) = 3.6. The addition of Ag/TNTs resulted in a slight shifting of the pH(*I*) to a more acidic range. The isoelectric point of the modified membranes ranged from 3.1 to 3.5 and it was similar to the pH(*I*) of the used nanocomposites (3.3 and 3.4 for Ag/TNT_2.5 and Ag/TNT_100, respectively). Kłodzińska et al. [50] reported that the pH(*I*) of living *E. coli* bacteria was around 2.4. This means that the bacteria cells possess positive charge only at very acidic conditions and in natural water or municipal wastewater their surface is negatively charged. Considering the differences in pH(*I*) values of bacteria and membranes, it can be assumed that the modified membranes, in case of which the difference is lower, may show better resistance to biofouling than the unmodified one.

3.5. Antimicrobial properties of Ag/TNTs-modified membranes

The antimicrobial properties of the unmodified (M1) and the Ag/TNTs-modified membranes (M2and M5) were evaluated at stirring conditions using a suspension of *E. coli* bacteria (see Section 2.7). The results are summarized in Fig. 9. The unmodified membrane (M1) did not show any noticeable antibacterial properties, the survival of *E. coli* was comparable with that observed for the blank test. Even the lowest concentration of Ag in Ag/TNTs added to the membrane significantly improved the antibacterial properties and for the M2 the degree of inhibition of *E. coli* growth amounted to ca. 21% in comparison with the control test. The highest antimicrobial activity was observed for the M5 membrane containing the highest concentration of silver in the NPs and

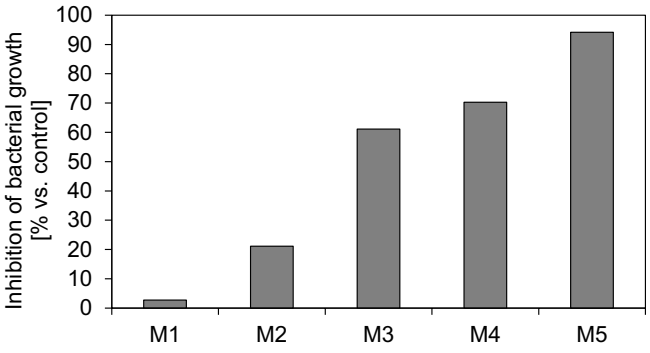

Fig. 9. The inhibition of *E. coli* growth by neat and Ag/TNT-modified PES membranes.

the bacterial growth was inhibited in that case for ca. 94%. Since the amount of Ag/TNTs in all membrane samples was the same, the observed differences were related to different concentration of Ag in the materials.

The course of changes of the antibacterial activity of the membranes can be related to Ag^+ leaching. The variations of silver concentration in saline solution after 1 and 7 d of incubation at 37°C are presented in Fig. 10. Similarly as in the case of Ag/TNT NPs (Fig. 2), an increase of silver concentration in the leaching solution with increasing Ag content in the nanomaterial was observed. Moreover, the leaching proceeded along with the duration of the experiment. The highest Ag concentration was observed after 7 d of experiment in case of M5 membrane (0.32 mg/dm^3). Nonetheless, the silver amount released during first 24 h was higher than the one observed during the next 6 d. The only difference was found for the M2 membrane, in case of which no progress in Ag release in time was observed. Taking into consideration the other membranes, it was found that the Ag amount released during the initial 24 h was 80%, 57%, and 63% of the total mass of the released silver for M3, M4, and M5, respectively. The kinetics of silver leaching from the membranes was consistent with the results obtained for NPs (Fig. 2) for which the highest Ag release from Ag/TNT_100 was observed during the first day of experiment.

Fig. 11 presents a comparison of SEM microphotographs of *E. coli* bacteria observed on a surface of the unmodified

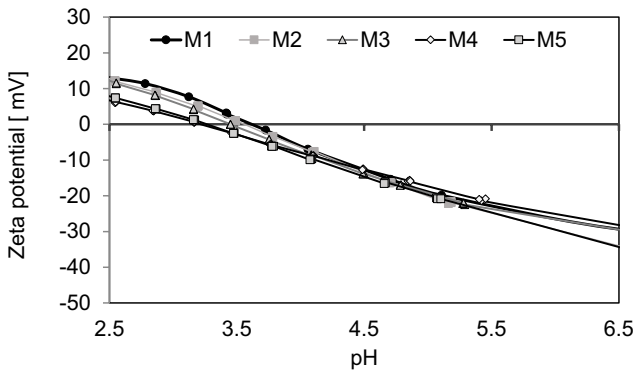

Fig. 8. Zeta potential of the Ag/TNTs-modified membranes.

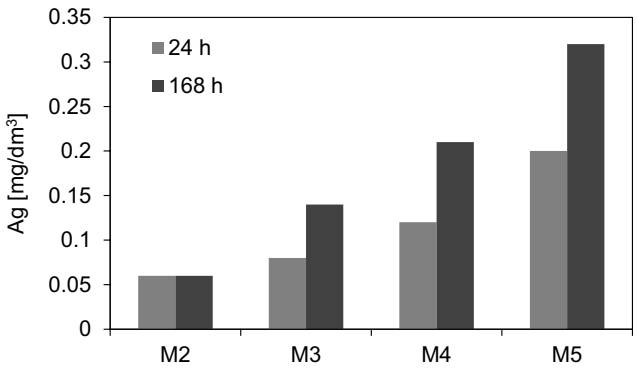

Fig. 10. Ag leaching from Ag/TNT-modified PES membranes; solution: 8.5 g NaCl/dm^3; temperature: 37°C.

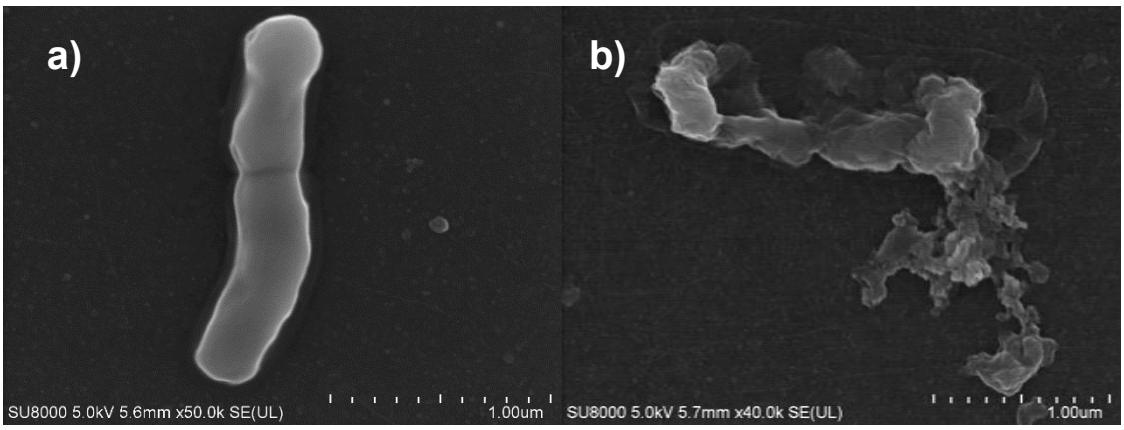

Fig. 11. SEM images of *E. coli* bacteria on the surface of (a) M1 and (b) M5 membrane after 40 h of exposition at stirring conditions.

M1 and the modified M5 membranes. The images confirmed the antibacterial activity of the membranes containing Ag/TNTs. A clearly visible damage of *E. coli* cell in case of M5 could be seen (Fig. 11(b)), accompanied by a release of the cellular content, which was further deposited on the membrane surface. Jung et al. [51] also observed a serious disruption of *E. coli* cells after 2 h exposition to silver ions solution of 0.2 mg/dm^3. The authors reported that the cells were cracked and ruptured, released their cellular content or in some cases a separation of the cell membrane from the cell wall took place.

Based on Fig. 12 a relationship between the presence of Ag/TNTs in the membrane structure and the inhibition of bacteria deposition on the membrane surface after 40 h of stirring was observed. The SEM-SE images (Fig. 12(a) and (c), left column) show that in case of the unmodified M1 membrane, the number of bacteria deposited on the surface was significantly higher than that observed in the presence of the Ag/TNTs-modified M5. The corresponding SEM-BSE images presented in Fig. 12(b) and (d) (right column) further suggest that the number of bacteria cells was especially low in the areas close to the NPs (light spots in the image).

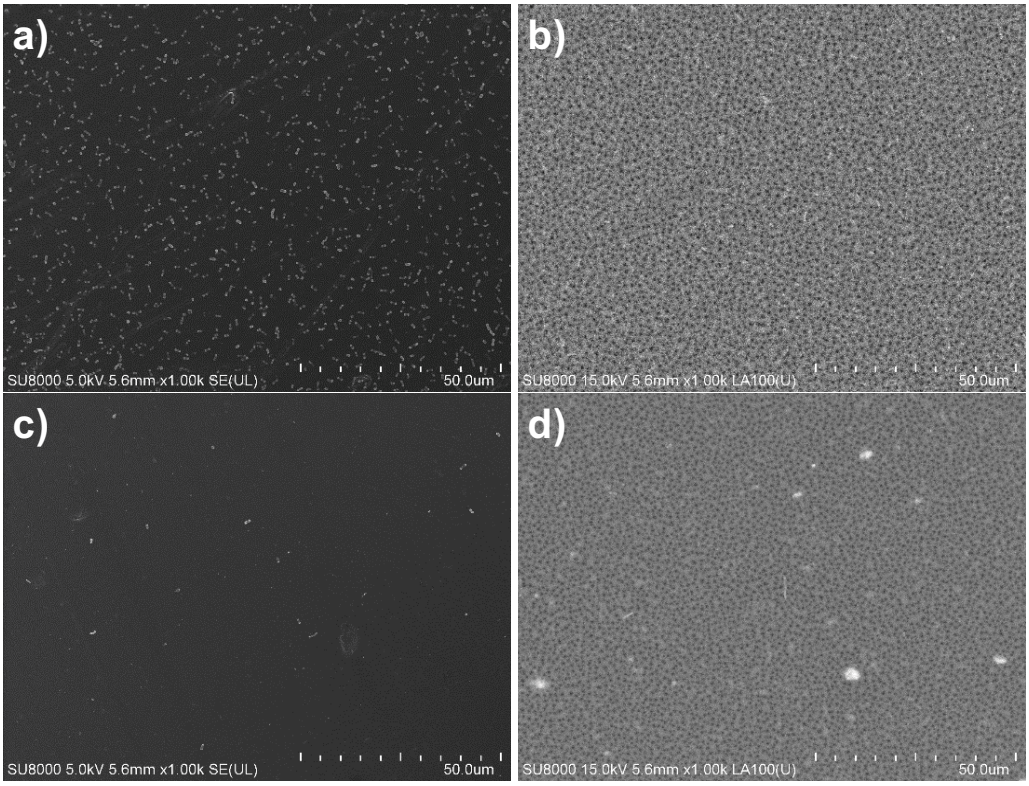

Fig. 12. SEM-SE ((a) and (c)) and SEM-BSE ((b) and (d)) images of the surface of: (a) and (b) M1 and (c) and (d) M5 membranes showing the influence of Ag/TNTs on *E. coli* bacteria presence.

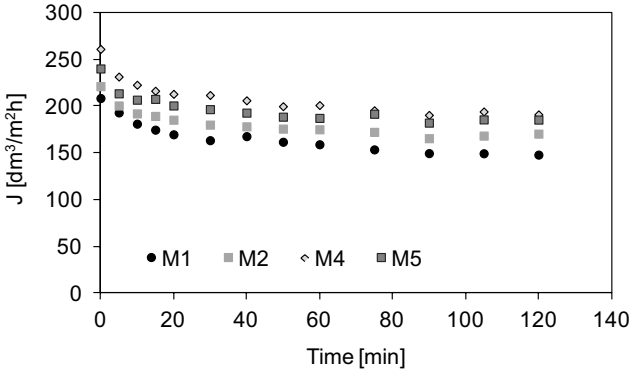

Fig. 13. Permeate fluxes during ultrafiltration of BSA solution (1 g/dm^3) through unmodified (M1) and Ag/TNTs-modified membranes (M2, M4, and M5); TMP = 2 bar.

3.6. Membrane fouling studies

The antifouling properties of the membranes were evaluated with application of BSA as a model foulant. Based on the PWF analysis (Fig. 4), the M1, M2, M4, and M5 membranes were selected for the fouling studies. The M3 membrane was not examined since the difference between the PWF determined for this membrane and the M2 was negligible. The permeate fluxes (J) measured during UF of BSA solution through the unmodified M1 membrane and the modified membranes are summarized in Fig. 13.

All of the modified membranes exhibited higher permeate fluxes than the unmodified one. The highest J values were observed for the M4 and M5 membranes, which was consistent with the PWF measurements (Fig. 4). The permeate flux during 2 h of UF of BSA solution in case of M2 was higher by ca. 15%, whereas in case of M4 and M5 – by ca. 29% and 25%, respectively, compared with the flux measured for M1. Analyzing the time-course changes of the fluxes, it was further observed that after 60 min the J values referred to the initial fluxes (J_0) were in the range of J/J_0 = 0.77–0.79 for M1 and M5, respectively, whereas after 120 min the J/J_0 ranged from 0.71 to 0.77, respectively. These data show that the rate of membrane fouling was higher in case of M1 membrane (23% flux decline after 1 h and 29% after 2 h) than in case of M5 one (21% and 23%, respectively). The obtained results confirm a positive effect of the modification of the PES membranes with Ag/TNTs on the mitigation of BSA membrane fouling. Furthermore, the data presented in Figs. 4 and 13 indicate that Ag content in the hybrid nanomaterial is of significant importance when both water permeability and fouling resistance are considered.

4. Conclusions

In this study the influence of addition of Ag/TNTs on physicochemical characteristics, antimicrobial properties, and fouling resistance of PES membranes was examined. A decrease of water contact angle values from 54° for unmodified M1 to 47°–48° for Ag/TNTs-modified M2–M5 confirmed a positive effect of the NPs on improvement of membranes hydrophilicity. The Ag/TNTs addition to PES membrane matrix resulted in slight shifting of the isoelectric point to more negative pH values (3.1–3.5) compared with the unmodified M1 membrane (3.6). No significant influence of the applied modification on the porosity of the membranes was noted, which was attributed to a relatively low loading of the NPs.

A significant improvement of PWF (ca. 15%–30%) compared with the neat M1 membrane was observed only in case of the membranes modified with Ag/TNTs containing high (11.44 or 23.21 wt%) concentration of Ag. The incorporation of the NPs to the membranes structure resulted in an increase of their antifouling properties. The permeate flux during UF of BSA solution was higher in case of the modified membranes than in case of the neat one for all the hybrid NPs used.

The incorporation of Ag/TNTs into PES membrane structure significantly improved its antimicrobial properties. The highest inhibition of *E. coli* growth (94% after 40 h of exposition) was observed in case of M5 membrane. The increasing antibacterial activity with increasing Ag content in the hybrid NPs was correlated with the silver ions leaching from the membranes. A relationship between Ag/TNTs presence in membranes matrix and the deposition and growth of bacteria on membranes surface was found. The number of *E. coli* bacteria on the surface of M1 was significantly higher than that observed in case of the Ag/TNTs-modified M5.

The research revealed a positive influence of modification with hybrid Ag/TNTs NPs on hydrophilicity, water permeability, fouling mitigation, and antibacterial properties of the fabricated mixed matrix PES membranes.

Acknowledgments

This work was supported by the National Science Centre, Poland under project no. 2016/21/B/ST8/00317. We would like to thank Prof. Zofia Lendzion-Bieluń for assistance with ICP-OES analysis. We would also like to thank BASF (Germany) for providing PES samples.

Symbols

B	—	Amount of bacteria determined in control sample, CFU/cm^3
C	—	Amount of bacteria determined in the presence of a membrane, CFU/cm^3
C_f	—	BSA concentration in feed, g/dm^3
C_p	—	BSA concentration in permeate, g/dm^3
I%	—	The percentage of the inhibition of bacterial growth with reference to the control (blank) sample, %
m_{wet}	—	The weight of membrane samples in the wet state, g
m_{dry}	—	The weight of membrane samples in the dry state, g
N	—	Number of bacteria colonies visible on Petri dish
R	—	Rejection, %
Y	—	Total dilution factor
Z	—	Volume of bacteria suspension put on the agar plate, 0.3 cm^3
ρ_w	—	Water density at 20°C, g/cm^3
ρ_p	—	PES density, g/cm^3

References

[1] R. Zhang, Y. Liu, M. He, Y. Su, X. Zhao, M. Elimelech, Z. Jiang, Antifouling membranes for sustainable water purification: strategies and mechanisms, Chem. Soc. Rev., 45 (2016) 5888–5924.

[2] D. Rana, T. Matsuura, Surface modifications for antifouling membranes, Chem. Rev., 110 (2010) 2448–2471.

[3] J. Zhu, J. Hou, Y. Zhang, M. Tian, T. He, J. Liu, V. Chen, Polymeric antimicrobial membranes enabled by nanomaterials for water treatment, J. Membr. Sci., 550 (2018) 173–197.

[4] A.K. Singh, P. Singh, S. Mishra, V.K. Shahi, Anti-biofouling organic-inorganic hybrid membrane for water treatment, J. Mater. Chem., 22 (2012) 1834–1844.

[5] Z. Wang, H. Wang, J. Liu, Y. Zhang, Preparation and antifouling property of polyethersulfone ultrafiltration hybrid membrane containing halloysite nanotubes grafted with MPC via RATRP method, Desalination, 344 (2014) 313–320.

[6] H. Yu, X. Zhang, Y. Zhang, J. Liu, H. Zhang, Development of a hydrophilic PES ultrafiltration membrane containing SiO_2@N-Halamine nanoparticles with both organic antifouling and antibacterial properties, Desalination, 326 (2013) 69–76.

[7] Y. Chen, Y. Zhang, J. Liu, H. Zhang, K. Wang, Preparation and antibacterial property of polyethersulfone ultrafiltration hybrid membrane containing halloysite nanotubes loaded with copper ions, Chem. Eng. J., 210 (2012) 298–308.

[8] S. Al Aani, V. Gomez, C.J. Wright, N. Hilal, Fabrication of antibacterial mixed matrix nanocomposite membranes using hybrid nanostructure of silver coated multi-walled carbon nanotubes, Chem. Eng. J., 326 (2017) 721–736.

[9] J. Wu, C. Yu, Q. Li, Novel regenerable antimicrobial nanocomposite membranes: effect of silver loading and valence state, J. Membr. Sci., 531 (2017) 68–76.

[10] J. Zhang, Y. Zhang, Y. Chen, L. Du, B. Zhang, H. Zhang, J. Liu, K. Wang, Preparation and characterization of novel polyethersulfone hybrid ultrafiltration membranes blending with modified halloysite nanotubes loaded with silver nanoparticles, Ind. Eng. Chem. Res., 51 (2012) 3081–3090.

[11] A. Gao, R. Hang, X. Huang, L. Zhao, X. Zhang, L. Wang, B. Tang, S. Ma, P.K. Chu, The effects of titania nanotubes with embedded silver oxide nanoparticles on bacteria and osteoblasts, Biomaterials, 35 (2014) 4223–4235.

[12] L. Wei, H. Wang, Z. Wang, M. Yu, S. Chen, Preparation and long-term antibacterial activity of TiO_2 nanotubes loaded with Ag nanoparticles and Ag ions, RSC Adv., 5 (2015) 74347–74352.

[13] H. Basri, A.F. Ismail, M. Aziz, Polyethersulfone (PES)–silver composite UF membrane: effect of silver loading and PVP molecular weight on membrane morphology and antibacterial activity, Desalination, 273 (2011) 72–80.

[14] I. Sawada, R. Fachrul, T. Ito, Y. Ohmukai, T. Maruyama, H. Matsuyama, Development of a hydrophilic polymer membrane containing silver nanoparticles with both organic antifouling and antibacterial properties, J. Membr. Sci., 387 (2012) 1–6.

[15] A. Mollahosseini, A. Rahimpour, M. Jahamshahi, M. Peyravi, M. Khavarpour, The effect of silver nanoparticle size on performance and antibacteriality of polysulfone ultrafiltration membrane, Desalination, 306 (2012) 41–50.

[16] H. Li, X.S. Shao, Q. Zhou, M.Z. Li, Q.Q. Zhang, The double effects of silver nanoparticles on the PVDF membrane: surface hydrophilicity and antifouling performance, Appl. Surf. Sci., 265 (2013) 663–670.

[17] M. Ben-Sasson, X. Lu, E.R. Bar-Zeev, K.S. Zodrow, S. Nejati, G.P. Qi, E. Giannelis, M. Elimelech, In situ formation of silver nanoparticles on thin-film composite reverse osmosis membranes for biofouling mitigation, Water Res., 62 (2014) 260–270.

[18] R. Liu, P. Wang, X. Wang, H. Yu, J. Yu, UV-and visible-light photocatalytic activity of simultaneously deposited and doped Ag/Ag (I)-TiO_2 photocatalyst, J. Phys. Chem. C, 116 (2012) 17721–17728.

[19] P.V. Viet, B.T. Phan, D. Mott, S. Maenosono, T.T. Sang, C.M. Thi, L.V. Hieu, Silver nanoparticle loaded TiO_2 nanotubes with high photocatalytic and antibacterial activity synthesized by photoreduction method, J. Photochem. Photobiol., A, 352 (2018) 106–112.

[20] B. Díez, N. Roldán, A. Martín, A. Sotto, J.A. Perdigón-Melón, J. Arsuaga, R. Rosal, Fouling and biofouling resistance of metal-doped mesostructured silica/polyethersulfone ultrafiltration membranes, J. Membr. Sci., 526 (2017) 252–263.

[21] J. Huang, H. Wang, K. Zhang, Modification of PES membrane with Ag–SiO_2: reduction of biofouling and improvement of filtration performance, Desalination, 336 (2014) 8–17.

[22] Y. Chen, Y. Zhang, H. Zhang, J. Liu, C. Song, Biofouling control of halloysite nanotubes-decorated polyethersulfone ultrafiltration membrane modified with chitosan-silver nanoparticles, Chem. Eng. J., 228 (2013) 12–20.

[23] J. Wu, C. Yu, Q. Li, Regenerable antimicrobial activity in polyamide thin film nanocomposite membranes, J. Membr. Sci., 476 (2015) 119–127.

[24] V. Vatanpour, A. Shockravi, H. Zarrabi, Z. Nikjavan, A. Javadi, Fabrication and characterization of anti-fouling and anti-bacterial Ag-loaded graphene oxide/polyethersulfone mixed matrix membrane, Ind. Eng. Chem. Res., 30 (2015) 342–352.

[25] J. Huang, G. Arthanareeswaran, K. Zhang, Effect of silver loaded sodium zirconium phosphate (nanoAgZ) nanoparticles incorporation on PES membrane performance, Desalination, 285 (2012) 100–107.

[26] H. Wang, L. Wei, Z. Wang, S. Chen, Preparation, characterization and long-term antibacterial activity of Ag–poly (dopamine)–TiO_2 nanotube composites, RSC Adv., 6 (2016) 14097–14104.

[27] B. Vijayan, N. Dimitrijevic, M.T. Rajh, K. Gray, Effect of calcination temperature on the photocatalytic reduction and oxidation processes of hydrothermally synthesized titania nanotubes, J. Phys. Chem. C, 114 (2010) 12994–13002.

[28] A. Patrón-Soberano, B.P. Núñez-Luna, S. Casas-Flores, A. De las Peñas, R.B. Domínguez-Espíndola, V. Rodríguez-González, Photo-assisted inactivation of *Escherichia coli* bacteria by silver functionalized titanate nanotubes, Ag/$H_2Ti_2O_5{\cdot}H_2O$, Photochem. Photobiol. Sci., 16 (2017) 854–860.

[29] V. Rodríguez-González, R.B. Domínguez-Espíndola, S. Casas-Flores, O.A. Patrón-Soberano, R. Camposeco-Solis, S.W. Lee, Antifungal nanocomposites inspired by titanate nanotubes for complete inactivation of *Botrytis cinerea* isolated from tomato infection, ACS Appl. Mater. Interfaces, 8 (2016) 31625–31637.

[30] M. Grandcolas, J. Ye, N. Hanagata, Combination of photocatalytic and antibacterial effects of silver oxide loaded on titania nanotubes, Mater. Lett., 65 (2011) 236–239.

[31] D. Guin, S.V. Manorama, J.N.L. Latha, S. Singh, Photoreduction of silver on bare and colloidal TiO_2 nanoparticles/nanotubes: synthesis, characterization, and tested for antibacterial outcome, J. Phys. Chem. C, 111 (2007) 13393–13397.

[32] F. Cesano, S. Bertarione, M.J. Uddin, G. Agostini, D. Scarano, A. Zecchina, Designing TiO_2 based nanostructures by control of surface morphology of pure and silver loaded titanate nanotubes, J. Phys. Chem. C, 114 (2009)169–178.

[33] M.S.L. Yee, P.S. Khiew, S.S. Lim, W.S. Chiu, Y.F. Tan, Y.Y. Kok, C.O. Leong, Enhanced marine antifouling performance of silver-titania nanotube composites from hydrothermal processing, Colloids Surf., A, 520 (2017) 701–711.

[34] M.N. Subramaniam, P.S. Goh, W.J. Lau, Y.H. Tan, B.C. Ng, A.F. Ismail, Hydrophilic hollow fiber PVDF ultrafiltration membrane incorporated with titanate nanotubes for decolourization of aerobically-treated palm oil mill effluent, Chem. Eng. J., 316 (2017) 101–110.

[35] M. Padaki, D. Emadzadeh, T. Masturra, A.F. Ismail, Antifouling properties of novel PSf and TNT composite membrane and study of effect of the flow direction on membrane washing, Desalination, 362 (2015) 141–150.

[36] I.H. Alsohaimi, M. Kumar, M.S. Algamdi, M.A. Khan, K. Nolan, J. Lawler, Antifouling hybrid ultrafiltration membranes with high selectivity fabricated from polysulfone and sulfonic acid functionalized TiO_2 nanotubes, Chem. Eng. J., 316 (2017) 573–583.

[37] A.K. Zulhairun, M.N. Subramaniam, A. Samavati, M.K.N. Ramli, M. Krishparao, P.S. Goh, A.F. Ismail, High-flux polysulfone mixed matrix hollow fiber membrane incorporating

mesoporous titania nanotubes for gas separation, Sep. Purif. Technol., 180 (2017) 13–22.
[38] I.W. Azelee, P.S. Goh, W.J. Lau, A.F. Ismail, M. Arzhandi, K.C. Wong, M.N. Subramaniam, Enhanced desalination of polyamide thin film nanocomposite incorporated with acid treated multiwalled carbon nanotube-titania nanotube hybrid, Desalination, 409 (2017) 163–170.
[39] B.L. He, B. Dong, H.L. Li, Preparation and electrochemical properties of Ag-modified TiO_2 nanotube anode material for lithium–ion battery, Electrochem. Commun., 9 (2007) 452–430.
[40] Q.L. Feng, J. Wu, G.Q. Chen, F.Z. Cui, T.N. Kim, J.O. Kim, A mechanistic study of the antibacterial effect of silver ions on *E. coli* and *Staphylococcus aureus*, J. Biomed. Mater. Res., 52 (2000) 662–668.
[41] M. Guzman, J. Dille, S. Godet, Synthesis and antibacterial activity of silver nanoparticles against gram-positive and gram-negative bacteria, Nanomedicine, 8 (2012) 37–45.
[42] A. Nazerah, A.F. Ismail, J. Jaafar, Incorporation of bactericidal nanomaterials in development of antibacterial membrane for biofouling mitigation: a mini review, J. Teknol. Sci. Eng., 78 (2016) 53–61.
[43] D.Y. Koseoglu-Imer, B. Kose, M. Altinbas, I. Koyuncu, The production of polysulfone (PS) membrane with silver nanoparticles (AgNP): physical properties, filtration performances, and biofouling resistances of membranes, J. Membr. Sci., 428 (2013) 620–628.
[44] X. Li, R. Pang, J. Li, X. Sun, J. Shen, W. Han, L. Wang, In situ formation of Ag nanoparticles in PVDF ultrafiltration membrane to mitigate organic and bacterial fouling, Desalination, 324 (2013) 48–56.
[45] Q. Chen, Z. Yu, Y. Pan, G. Zeng, H. Shi, X. Yang, F. Li, S. Yang, Y. He, Enhancing the photocatalytic and antibacterial property of polyvinylidene fluoride membrane by blending Ag–TiO_2 nanocomposites, J. Mater. Sci. – Mater. Electron., 28 (2017) 3865–3874.
[46] K. Zodrow, L. Brunet, S. Mahendra, D. Li, A. Zhang, Q. Li, P.J.J. Alvarez, Polysulfone ultrafiltration membranes impregnated with silver nanoparticles show improved biofouling resistance and virus removal, Water Res., 43 (2009) 715–723.
[47] L. Huang, S. Zhao, Z. Wang, J. Wu, J. Wang, S. Wang, In situ immobilization of silver nanoparticles for improving permeability, antifouling and anti-bacterial properties of ultrafiltration membrane, J. Membr. Sci., 499 (2016) 269–281.
[48] M. Zhang, K. Zhang, B. De Gusseme, W. Verstraete, Biogenic silver nanoparticles (bio-Ag^0) decrease biofouling of bio-Ag^0/PES nanocomposite membranes, Water Res., 46 (2012) 2077–2087.
[49] A. Sotto, A. Boromand, S. Balta, J. Kim, B. Van der Bruggen, Doping of polyethersulfone nanofiltration membranes: antifouling effect observed at ultralow concentrations of TiO_2 nanoparticles, J. Mater. Chem., 21 (2011) 10311–10320.
[50] E. Kłodzińska, M. Szumski, E. Dziubakiewicz, K. Hrynkiewicz, E. Skwarek, W. Janusz, B. Buszewski, Effect of zeta potential value on bacterial behavior during electrophoretic separation, Electrophoresis, 31 (2010) 1590–1596.
[51] W.K. Jung, H.C. Koo, K.W. Kim, S. Shin, S.H. Kim, Y.H. Park, Antibacterial activity and mechanism of action of the silver ion in *Staphylococcus aureus* and *Escherichia coli*, Appl. Environ. Microbiol., 74 (2008) 2171–2178.